PHYSICAL REVIEW E VOLUME 55, NUMBER 5 MAY 1997

Competition between spiral-defect chaos and rolls in Rayleigh-Bénard convection

Kapil M. S. Bajaj, David S. Cannell, and Guenter Ahlers
Department of Physics and Center for Nonlinear Science, University of California, Santa Barbara, California 93106
(Received 4 December 1996)

We present experimental results for pattern formation in the Rayleigh-Bénard convection of a fluid with a Prandtl number $\sigma \simeq 4$. We find that the spiral-defect-chaos (SDC) attractor, which exists for $\sigma \simeq 1$, has become unstable. Gradually increasing the temperature difference ΔT from below to well above its critical value ΔT_c no longer leads to SDC. A sudden jump of ΔT from below to above ΔT_c causes convection to grow from fluctuations and does yield SDC. However, the SDC is a transient; it coarsens and forms a single cell-filling spiral which then drifts toward the cell wall and disappears. [S1063-651X(97)50105-X]

PACS number(s): 47.54.+r, 47.20.Lz, 47.27.Te, 47.52.+j

Rayleigh-Bénard convection (RBC) occurs in a shallow horizontal layer of a fluid heated from below when the temperature difference ΔT across the layer exceeds a critical value ΔT_c. The velocity fields which form above ΔT_c have long been used as an experimental testing ground for theories of pattern formation in nonlinear systems [1]. The phenomena which occur depend upon the Prandtl number $\sigma = \nu/\kappa$, the dimensionless ratio of the kinematic viscosity ν to the thermal diffusivity κ. A fascinating recent discovery in RBC is that of spiral-defect chaos (SDC) for $\sigma \simeq 1$ [2]. It consists of patches of rotating convection-roll spirals and of other defects, and occurs for $\epsilon \equiv \Delta T/\Delta T_c - 1 > \epsilon_s > 0$. The spirals are coherent structures with a typical diameter of a few roll wavelengths. They can be right- or left-handed, single- or multiarmed, and appear and disappear irregularly in time and space. SDC has since been found in numerical solutions of model equations [3] and of the Navier-Stokes equations (NSE) [4]. The band of wave numbers for SDC [2,4] lies well within the range for which straight rolls are also stable [5] in the laterally infinite system. Thus the solutions of the equations of motion of the RBC exhibit bistability of time-independent straight rolls and of SDC, with each of the two having distinct attractor basins. For $\sigma \lesssim 1$ the generic initial conditions of real RBC experiments lie in the attractor basin of SDC [2,6]. Here we report that this situation is changed dramatically when σ is increased. For $\sigma = 4.0 \pm 0.2$, we do not find any spirals when increasing ϵ in small steps from below zero to large positive values. Thus this experimental path does not cross an attractor basin of SDC. However, when ϵ is increased suddenly from below zero to values of $O(1)$, SDC evolves in the sample interior from random noise [7]. Thus random initial conditions appear to remain within the attractor basin of SDC even for $\sigma \simeq 4$. But this is illusory since the SDC turns out to be a transient rather than a stable attractor. At very long times, the spirals coarsen, forming larger and larger spirals until only one giant spiral fills nearly the entire cell. At even longer times the giant spiral is not stable either; its head slowly drifts toward the sidewall and disappears from the cell, leaving a state similar to those obtained by increasing ϵ gradually. Our observations differ from those of Assenheimer and Steinberg [8,9], who reported SDC in a sample of SF_6 near its critical point with Prandtl numbers similar to and even larger than ours.

A detailed description of the apparatus was given in Ref. [10]. The convection cell had a 0.95 cm thick sapphire top plate and a diamond-machined aluminum bottom plate. A film heater glued to the lower side of the bottom plate provided the heat current. The top of the sapphire plate was in contact with a temperature-regulated circulating water bath. The temperatures for both bottom and top plates were regulated to better than 1 mK. The circular sidewall was made of high-density polyethylene. It had an inner diameter of 8.89 cm, and was sealed to the top and bottom plates with ethylene-propylene O-rings. High-purity liquid-chromatography grade acetone was dried by using 3 Å molecular sieves followed by distillation, and then injected into the cell with a syringe without significant exposure to the atmosphere. Two cells were used. The cell height was $d = 0.80 \pm 0.01$ (1.0 ± 0.01) mm, corresponding to an aspect ratio (radius/height) $\Gamma \approx 55$ (45). The calculated value of ΔT_c was 8.56 (4.50) °C. At onset, the coefficient Q [11] describing the departure from the Boussinesq approximation was 0.37 (0.20). The vertical thermal diffusion time t_v was 6.8 (10.5) s. The onset of convection was determined from measurements of the Nusselt number $\mathcal{N}$ (the ratio of the effective thermal conductivity to that in the conduction state). Quasistatic results for $\mathcal{N}$ over the entire range of the experiment are shown in Fig. 1. Images of convection patterns were taken using the shadowgraph apparatus described previously [12].

In one set of experiments, ϵ was varied slowly from below 0 to above 5 by changing it in steps of about 0.1. The

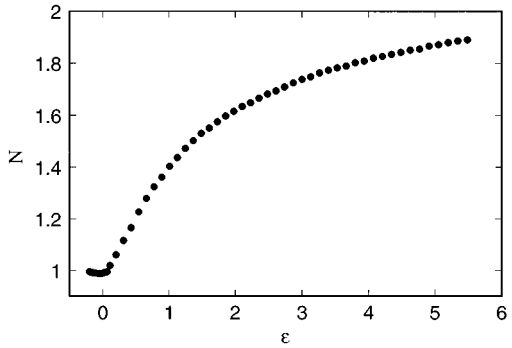

FIG. 1. The Nusselt number $\mathcal{N}$ vs ϵ for $\Gamma = 45$ obtained while increasing ϵ quasistatically. For this run, the top temperature was 16.5 °C and $\Delta T_c = 4.50$ °C.

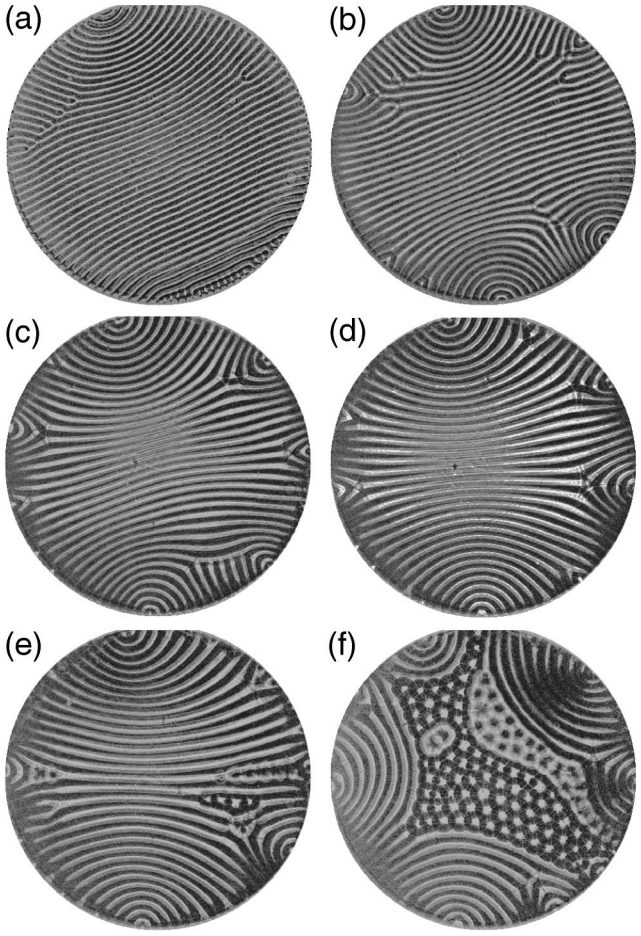

FIG. 2. Representative images obtained during the experimental run of Fig. 1 where ϵ was increased gradually. (a) $\epsilon=0.5$; (b) $\epsilon=2.0$; (c) $\epsilon=3.7$; (d) $\epsilon=4.5$. Up to this value of ϵ, ''rolls'' (with curvature, wall foci, etc.) are stable and time independent. Images (e) and (f) are for $\epsilon=5.0$, $1000t_v$, and $6000t_v$ after increasing ϵ. They show the coexistence of hexagon domains with upflow and downflow at the cell centers and with rolls and wall foci. No spirals or targets were encountered.

system was allowed to equilibrate for at least one horizontal diffusion time $\Gamma^2 t_v$ (about 6 h) after each step. This procedure corresponds to an effective ramp rate $\beta \equiv d\epsilon/dt \leq 5.4\times 10^{-5}$ (here t is measured in units of t_v). It yielded images like those shown in Fig. 2. For $\epsilon \lesssim 1$, the patterns consisted essentially of straight rolls, except for typically one or two grain boundaries and perhaps one focus singularity adjacent to the sidewall. A representative example is shown in Fig. 2(a), which is for $\epsilon=0.5$. The wide range of ϵ over which relatively straight rolls occur is in contrast to the $\sigma \simeq 1$ case, where significant roll curvature occurs already for $\epsilon \gtrsim 0.1$ [13,14]. Figures 2(b), 2(c), and 2(d) are for $\epsilon=$ 2.0, 3.7, and 4.5. They show that the rolls do acquire significant curvature as ϵ is increased. This curvature is associated with a tendency for the roll axes to terminate perpendicular to the wall. It leads to the formation of additional wall foci and to a reduction of the roll wavelength in the cell center. For $\sigma \simeq 1$, this phenomenon occurred already at ϵ values which were about an order of magnitude smaller, and yielded a time-dependent state with repeated formation of defects in the cell interior via the skewed-varicose mechanism [13,14].

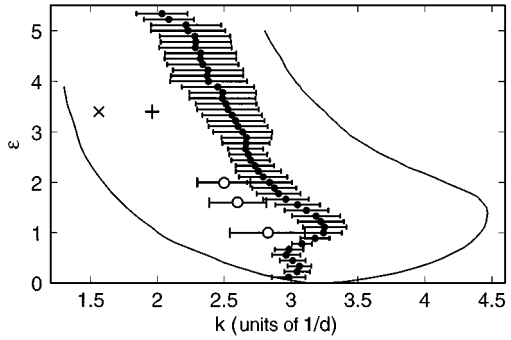

FIG. 3. The solid circles are the mean wave vectors obtained in the run of Fig. 1 by increasing ϵ quasistatically for $\Gamma=45$. The open circles are wave vectors obtained from the SDC state before the coarsening process had progressed significantly. The horizontal bars through the data points correspond to the width of the structure function $S(k)$. The plus and cross are the wave vectors reported in Ref. [9] for rolls and hexagons, respectively. The solid line is the stability boundary for straight rolls in the laterally infinite system.

In the present case, the images were essentially independent of time at constant ϵ. No defect formation occurred because even the significantly enhanced wave-number range encountered in the cell interior did not result in any crossing of the skewed-varicose instability boundary. We illustrate this latter point in Fig. 3, which at small wave numbers gives the Eckhaus and at large wave numbers the skewed-varicose instability as a solid line. The solid circles are the mean wave numbers k from the present run. They were obtained from the structure functions $S(k)$ (squares of the moduli of the Fourier transforms) of the images as described elsewhere [2]. The horizontal bars represent the widths of the structure functions, obtained from the second moments of $S(k)$ about $\overline{k}$. It is apparent from these data that even the large- and small-k tails of $S(k)$ are primarily well within the range of stable straight rolls of the infinite system.

When ϵ was increased further, the formation of cellular flow began near one of the wall foci, as shown in Fig. 2(e) for $\epsilon=5.0$. During many horizontal diffusion times these flow cells multiplied and spread over a wider part of the sample and evolved into a pattern of coexisting regions of hexagons with either upflow or downflow at their centers. These regions occurred together with curved rolls and wall foci in other parts of the sample. This is shown in Fig. 2(f), which is also for $\epsilon=5.0$ but $6000t_v$ after ϵ was last increased. This pattern is similar to ones observed by Assenheimer and Steinberg [9] (AS) with SF_6 close to its gas-liquid critical point in a cell with $\Gamma=80$ at $\epsilon=3.4$ and $\sigma=4.5$. However, the threshold for and mechanism of hexagon generation seems different in our case, since AS report that their hexagons appear already near $\epsilon=2.8$, and via a core instability of spirals or targets which do not exist in our system. Apparently the threshold for hexagon generation depends on the nature of the previously existing structure.

Of greatest relevance to the present issue is that none of the images obtained in runs like the one described above revealed any spirals. This is so also for the larger $\Gamma=55$. In contrast to this, for $\sigma \simeq 1$ and similar values of Γ [14,6] the onset of SDC was found at $\epsilon_s \simeq 0.55$, and SDC persisted to above $\epsilon \simeq 3$ where the oscillatory instability was encountered

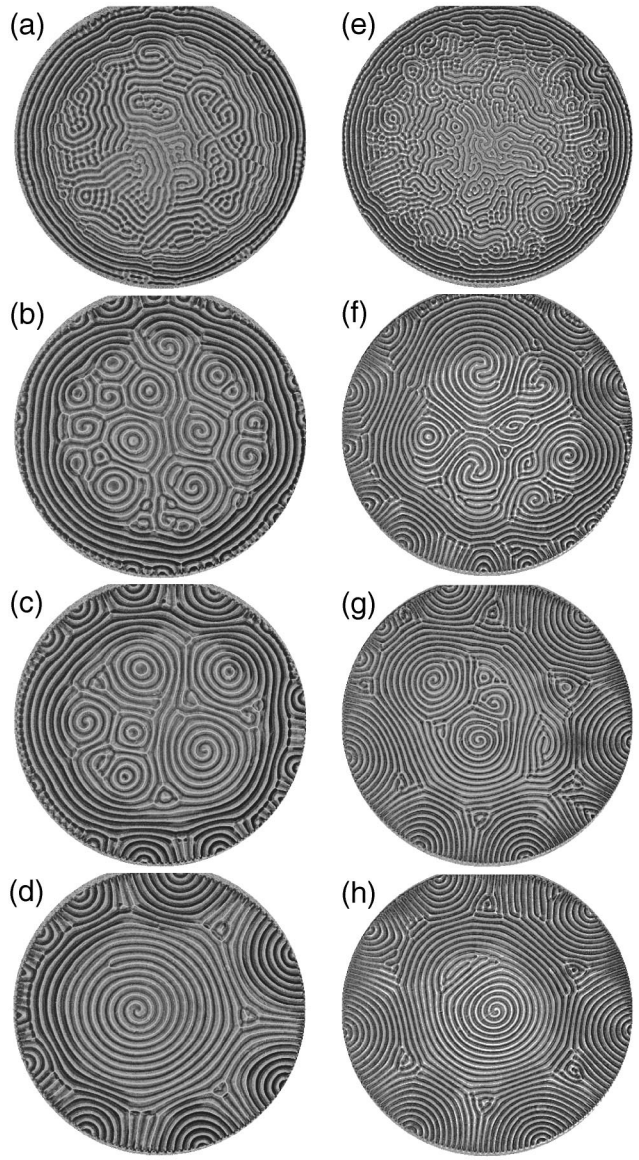

FIG. 4. The time evolution of the patterns after changing ϵ suddenly from $\epsilon_0=-1$ to $\epsilon_1>0$. Images (a)–(d) are for $\Gamma=45$ and $\epsilon_1=2.0$ with a top temperature of 16.5 °C and $\Delta T_c=4.50$ °C. In units of $t_v=10.5$ s, the elapsed times since the jump in ϵ are (a) $t=2$, (b) $t=400$, (c) $t=2000$, and (d) $t=8000$. Images (e)–(h) are for $\Gamma=55$ and $\epsilon_1=1.0$ with a top temperature of 19.0 °C and $\Delta T_c=8.56$ °C. In units of $t_v=6.8$ s, the elapsed times since the jump in ϵ are (e) $t=2$, (f) $t=600$, (g) $t=6000$, and (h) $t=10000$. In both examples the pattern in the cell interior developed from random convective flows, and the spiral-target structures coarsened and healed to a single spiral and some defects along the wall over a few horizontal diffusion times $\Gamma^2 t_v$.

at that σ value. The total absence of spirals in our experiment also differs from the results reported by AS, who for $\sigma=4.3$ found spirals and targets (zero-armed spirals) for $\epsilon\gtrsim 0.84$.

In a second set of experiments we increased ϵ suddenly from $\epsilon_0=-1$ to $\epsilon_1>0$. Care was taken to increase ϵ as quickly as possible to the final value in a smooth, monotonic manner without overshooting. This procedure yielded small-amplitude random convective flows in the cell center after only a few t_v. Examples are shown in Figs. 4(a) and 4(e).

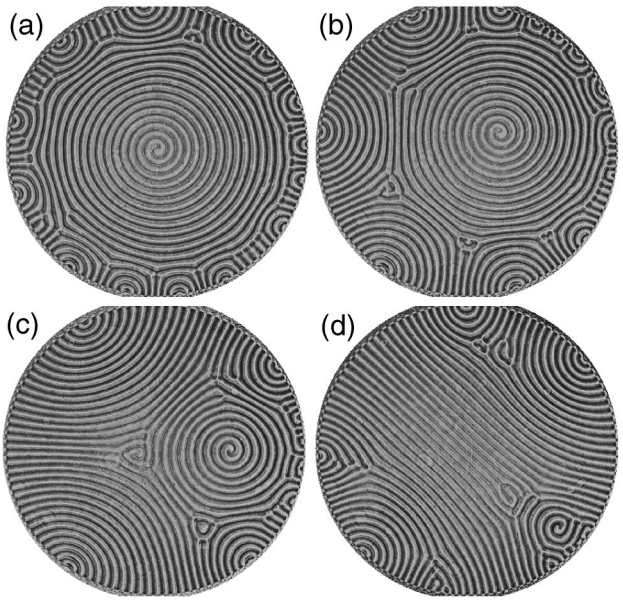

FIG. 5. The long-time evolution of the patterns after changing ϵ suddenly from $\epsilon_0=-1$ to $\epsilon_1=1.6$ for $\Gamma=45$. For this run, the top temperature was 18.0 °C, and $\Delta T_c=4.53$ °C. The elapsed times (in units of t_v) since the jump in ϵ are (a) $t=7500$, (b) $t=19\,000$, (c) $t=30\,000$, and (d) $t=38\,000$.

The dynamic sidewall forcing during the transient typically led to a small number of concentric rolls surrounding the random flow field in the center. Stabilizing at various values of $\epsilon_1\gtrsim 1$, we observed a rapid growth (typically within $30t_v$) of targets and spirals from the disordered flow field, as shown in Figs. 4(b) and 4(f). Simultaneously the mean wave vector decreased and after a relatively short time settled down at the points shown by the open circles in Fig. 3. Once the pattern of spirals, targets, and other defects was generated, the complicated dynamics of SDC, known from the experiments at smaller σ, came into play. For smaller ϵ_1 (say $\epsilon_1\simeq 0.5$), no spirals or targets developed and a pattern like that of Fig. 2(a) evolved after a relatively short time.

In contrast to the experiments with $\sigma\simeq 1$, the SDC state which for $\epsilon_1\gtrsim 1$ grew from the random initial conditions was not stable. Instead of persistent SDC dynamics, we observed a coarsening of the patterns over time. This is illustrated by Figs. 4(c) and 4(g). The spirals grew in size until after a few horizontal diffusion times there was left primarily one giant, nearly cell filling, slowly rotating spiral as shown in Figs. 4(d) and 4(h).

Although the giant spirals lived for several horizontal diffusion times, experiments over even longer times showed that they were not really stable. This is illustrated in Fig. 5. At $7500t_v$ after a jump in ϵ to $\epsilon_1=1.6$, one giant spiral is positioned with its core centered in the cell. As shown by the other images, this core location is not stable; the core gradually drifts towards the wall while the radius of the spiral decreases so that it roughly equals the distance of the core from the wall. During this process, no new spirals or targets are born. At a time shortly after that of image 5(d), the core left the cell altogether and a state of straight-curved rolls and wall foci similar to the ones obtained by the slow increase of ϵ (Fig. 2) remained.

For $\sigma\simeq 4$ and $\Gamma=45$ or 55, we found that SDC can be

attained from the random flow fields generated by a jump in ϵ, but not by quasistatic changes of ϵ. This is in contrast to $\sigma \lesssim 1$, where SDC is difficult to avoid for $\Gamma \gtrsim 30$ [2,6] no matter how ϵ is varied. We also demonstrated by experiments extending over very long times that SDC, once formed, is unstable in our samples with $\sigma \simeq 4$. It coarsens and evolves into a single cell-filling spiral, whose core then drifts from the cell center towards the sidewall where it disappears. Our results differ from those of Assenheimer and Steinberg [8,9], who found SDC without coarsening over the wide range $2.8 \lesssim \sigma \lesssim 28$, with the spirals gradually being replaced by targets as σ increases. The reason for this difference is unclear. However, we note several differences between the two experiments. In one run with $\sigma = 4.5$ described by AS in some detail [9], they used a cell for which ΔT_c was two orders of magnitude smaller than ours. Thus, assuming that their temperature control was similar to ours, their experimental noise (spatial as well as temporal) in ϵ presumably was two orders of magnitude larger than ours. Furthermore, extremely slow ramp rates $\beta \simeq 5 \times 10^{-5}$ like ours would be more difficult to attain when ΔT_c is very small. Also, the total time intervals over which they observed SDC at constant ϵ were only $O(\Gamma^2 \tau_v)$ [15] and are at least an order of magnitude smaller than ours ($\approx 18 \Gamma^2 t_v$). Finally we note that AS used a sample with $\Gamma = 80$ which is a factor of 1.5 larger than one of ours. One might conjecture that larger Γ ($= 80$, the AS value) stablizes SDC for $\sigma \simeq 4$, whereas $\Gamma = 55$ (our larger value) destabalizes it. This would require a strong σ dependence of $\epsilon_s(\sigma, \Gamma)$ because SDC is readily attained, for instance, for $\Gamma = 30$ and $\sigma = 1$. If this trend in σ dependence continues for $\sigma > 4$, AS should not have observed SDC in their cell with $\Gamma = 80$ at their much higher Prandtl numbers, up to 20 or larger. We conclude that the differences between the two experiments remain unresolved, and that additional measurements, particularly as a function of Γ, are required to shed light on this problem. Unfortunately it is difficult to reach larger Γ values using acetone because ΔT_c becomes very large if d is reduced.

Finally we remark that it would be interesting to search for the coarsening and instability of SDC in solutions of the Navier-Stokes equations.

We are grateful to Werner Pesch for permitting us to use his program and for his advice during the calculation of the stability boundary in Fig. 3. This work was supported by the National Science Foundation through Grant No. DMR94-19168.

[1] M. C. Cross and P. C. Hohenberg, Rev. Mod. Phys. **65,** 851 (1993).

[2] S. W. Morris, E. Bodenschatz, D. S. Cannell, and G. Ahlers, Phys. Rev. Lett. **71,** 2026 (1993).

[3] H.-W. Xi, J. D. Gunton, and J. Vinals, Phys. Rev. Lett. **71,** 2030 (1993); M. C. Cross and Y. Tu, *ibid.* **75,** 834 (1995).

[4] W. Decker, W. Pesch, and A. Weber, Phys. Rev. Lett. **73,** 648 (1994).

[5] F. H. Busse and R. M. Clever, J. Fluid Mech. **91,** 319 (1979); F. H. Busse, in *Hydrodynamic Instabilities and the Transition to Turbulence*, edited by H. Swinney and J. P. Gollub (Springer-Verlag, Berlin, 1981), p. 97.

[6] J. Liu and G. Ahlers, Phys. Rev. Lett. **77,** 3126 (1996).

[7] M. Wu, G. Ahlers, and D. S. Cannell, Phys. Rev. Lett. **75,** 1743 (1995).

[8] M. Assenheimer and V. Steinberg, Nature (London) **367,** 345 (1994).

[9] M. Assenheimer and V. Steinberg, Phys. Rev. Lett. **76,** 756 (1996).

[10] M. D. Dominguez-Lerma, G. Ahlers, and D. S. Cannell, Phys. Rev. E **52,** 6159 (1995).

[11] F. Busse, J. Fluid Mech. **30,** 625 (1967).

[12] J. R. de Bruyn, E. Bodenschatz, S. W. Morris, S. Trainoff, Y. Hu, D. S. Cannell, and G. Ahlers, Rev. Sci. Instrum. **67,** 2043 (1996).

[13] V. Croquette, Contemp. Phys. **30,** 153 (1989).

[14] Y. Hu, R. E. Ecke, and G. Ahlers, Phys. Rev. E **51,** 3263 (1995).

[15] M. Assenheimer, Ph. D. thesis, The Weizmann Institute of Science, 1994.